Nuclear Engineering and Technology 52 (2020) 552–559

Contents lists available at ScienceDirect

Nuclear Engineering and Technology

journal homepage: www.elsevier.com/locate/net

Original Article

Second order integral sliding mode observer and controller for a nuclear reactor

Piyush V. Surjagade [a, *], S.R. Shimjith [a, b], A.P. Tiwari [a, c]

[a] Homi Bhabha National Institute, Mumbai, 400094, India
[b] Reactor Control System Design Section of Bhabha Atomic Research Centre, Trombay, Mumbai, 400085, India
[c] Human Resource Development Division of Bhabha Atomic Research Centre, Trombay, Mumbai, 400085, India

ARTICLE INFO

Article history:
Received 7 December 2018
Received in revised form
23 May 2019
Accepted 18 August 2019
Available online 23 August 2019

Keywords:
Optimal control
Sliding mode control
Sliding mode observer
Nuclear reactor

ABSTRACT

This paper presents an observer-based chattering free robust optimal control scheme to regulate the total power of a nuclear reactor. The non-linear model of nuclear reactor is linearized around a steady state operating point to obtain a linear model for which an optimal second order integral sliding mode controller is designed. A second order integral sliding mode observer is also designed to estimate the unmeasurable states. In order to avoid the chattering effect, the discontinuous input of both observer and controller are designed using the super-twisting algorithm. The proposed controller is realized by combining an optimal linear tracking controller with a second order integral sliding mode controller to ensure minimum control effort and robustness of the closed-loop system in the presence of uncertainties. The condition for the selection of gains of discontinuous control based on the super-twisting algorithm is derived using a strict Lyapunov function. Performance of the proposed observer based control scheme is demonstrated through non-linear simulation studies.

1. Introduction

Power control is a challenging task in nuclear reactors due to their inherent non-linear and time varying nature, where the system parameters vary with operating power level and fuel burnup. In practice, reactor dynamics is always influenced by system uncertainties including parameter uncertainties, unmodeled dynamics, and external disturbances. Therefore, a simple and high performance robust control strategy, which ensures satisfactory performance and closed-loop stability in the presence of system uncertainties, is preferable for a nuclear reactor. In recent past, various adaptive and robust control schemes [1–7] have been developed to tackle the uncertainties present in the system. However, while handling the system uncertainties and at the same time maintaining the acceptable system performance robust controller often spend high control energy. Thus, a robust control strategy which uses less control energy is always preferable.

Design of control system using optimal control technique guarantees the optimal performance with minimum control efforts [8]. However, in an uncertain environment, the performance of the optimal controller may become unsatisfactory, because, at the time of controller design, these control design techniques do not consider any uncertainties present in the system. Thus, to improve the performance of optimal controller in the presence of uncertainties, researchers have combined it with the robust controller thereby making a new control strategy known as hybrid control strategy [9].

Among different robust control design techniques, Sliding Mode Control (SMC) has been the most widely used in various applications because of its inherent robustness towards matched uncertainties [10]. In the SMC system, as soon as the system states reach the well defined sliding surface the matched uncertainties are completely eliminated, but during reaching phase system is sensitive to uncertainties. Therefore, to make the conventional SMC system more robust by eliminating the reaching phase, the concept of Integral Sliding Mode Control (ISMC) was proposed [11]. Thus, in the ISMC system, robustness is guaranteed throughout the system response.

Main obstacle in practical implementation of SMC techniques is the chattering effect which is characterized by high frequency oscillations around the sliding surface. In literature, various

* Corresponding author.,
E-mail addresses: piyush09.iitg@gmail.com, piyushvs@barc.gov.in (P.V. Surjagade), srshim@barc.gov.in (S.R. Shimjith), aptiwari@barc.gov.in (A.P. Tiwari).

https://doi.org/10.1016/j.net.2019.08.013
1738-5733/

techniques such as boundary layer technique, Second Order Sliding Mode (SOSM) technique, *etc* are proposed to overcome this problem (see Ref. [12] and references cited therein). The boundary layer technique suffers from the degradation of system performance and robustness. SOSM technique provides a potential solution to reduce the chattering without affecting the system performance and robustness. However, increasing information demand in terms of first time derivative of the sliding surface is the main problem of SOSM technique. The Super-Twisting Algorithm (STA) is a modified SOSM technique that does not require the information of any derivative of the sliding variable [13].

In the past, many control strategies based on state feedback are developed for nuclear reactor with the assumption that the state information is available [2,3,14]. Performance of such controllers depends significantly on accurate knowledge of the system states, though in practice, some of the states are not directly available for feedback. In a nuclear reactor, in particular, delayed neutron precursors' concentration are not directly measurable. Therefore, an observer is needed to estimate the unmeasurable states. In some circumstances, observer can also provide better estimates of measurable states that are contaminated by noise [15]. In recent years, state observation using sliding mode technique [7,15–18] is gaining much importance because of its insensitivity towards parameter variations and external disturbances, high accuracy, and finite time convergence compared to conventional observers.

In this paper, a new control strategy named Optimal Second Order Integral Sliding Mode Control (OSOISMC) is proposed. The overall controller is developed by combining the optimal Linear Quadratic Tracking (LQT) controller with robust second order ISMC. The OSOISMC ensures robustness towards matched uncertainties from the very beginning of the system response. In order to avoid the chattering effect, the discontinuous control is designed based on STA. Although STA based controllers have been studied for the nuclear reactors in Refs. [5,6], but, to the best of our knowledge, no studies have been conducted on the selection of gains of the super-twisting controller and its Lyapunov function based stability. Further, in this work, the relationship between the discontinuous control gains and the upper bound of derivative of lumped system uncertainties has been derived by defining a strict Lyapunov function. As proposed controller uses state feedback, a Second Order Integral Sliding Mode Observer (SOISMO) is also designed based on STA to estimate the unmeasurable states. The proposed observer based control scheme is then applied to regulate the total power of a Pressurized Heavy Water Reactor (PHWR).

Outline of this paper is as follows. Section II describe the PHWR model and its state space representation. In Section III, SOISMO is designed to estimate the unmeasurable states. Design procedure of OSOISMC is discussed in Section IV. Effectiveness of the proposed control scheme is demonstrated in Section V by simulation results. Conclusions are drawn in Section VI.

2. PHWR model and its state space representation

2.1. PHWR model

Detailed description of 540 MWe PHWR model can be found in Ref. [3]. There, reactor is described by point kinetics model in which power and delayed neutron precursor concentration variables are normalized to their respective full power values. The following set of differential equations represents the PHWR model

$$\frac{dP}{dt}=\frac{\rho-\sum_{i=1}^{6}\beta_i}{\ell}P+\sum_{i=1}^{6}\frac{\beta_i}{\ell}C_i, \tag{1}$$

$$\frac{dC_i}{dt}=\lambda_i P-\lambda_i C_i,\ (i=1,2,\ldots,6), \tag{2}$$

$$\rho=-k_z(H-H_0), \tag{3}$$

$$\frac{dH}{dt}=-m_z v, \tag{4}$$

where

P reactor power in fractional full power (FFP)
C_i delayed neutron precursor density for i^{th} group (FFP)
β_i delayed neutron fraction for i^{th} group
λ_i decay constant for i^{th} group (s^{-1})
ℓ prompt neutron lifetime (s)
ρ reactivity
H average water level of Zonal Control Compartments (ZCCs) (cm)
v input voltage signal to ZCC (V)
k_z constant
m_z constant

Values of constants used in equations (1)–(4) are given in Table 1.

2.2. State space representation

Linearizing the set of equations (1)–(4) around steady state operating point, and defining the state vector, input, and output vector respectively as

$$\begin{aligned} x&=[\,\delta P\ \delta H\ \delta C_1\ \delta C_2\ \delta C_3\ \delta C_4\ \delta C_5\ \delta C_6\,]^\top,\\ u&=\delta v,\\ y&=[\,\delta P\ \delta H\,]^\top, \end{aligned} \tag{5}$$

where δ denotes an incremental change, system can be represented in standard state space form as

$$\begin{aligned} \dot{x}(t)&=Ax(t)+Bu(t)\\ y(t)&=Mx(t), \end{aligned} \tag{6}$$

where $A\in\mathbb{R}^{8\times8}$ is the system matrix, $B\in\mathbb{R}^{8}$ is the input matrix, and $M\in\mathbb{R}^{2\times8}$ is the output matrix. A, B, and M are sparse matrices with

$$\begin{aligned} A_{(1,1)}&=\frac{\rho(0)-\sum_{i=1}^{6}\beta_i}{\ell},\\ A_{(1,2)}&=-\frac{k_zP(0)}{\ell},\\ A_{(1,2+i)}&=\frac{\beta_i}{\ell}, i=1,2,\ldots,6.\\ A_{(2+i,1)}&=\lambda_i, i=1,2,\ldots,6.\\ A_{(2+i,2+i)}&=-\lambda_i, i=1,2,\ldots,6\\ B_{(2)}&=-m_z,\\ M_{(1,1)}&=1,\\ M_{(2,2)}&=1, \end{aligned}$$

and all the remaining elements zero. It can be observed that, with

Table 1
Values of constants and delayed neutron data for 540 MWe PHWR.

$\beta_1 = 0.1611 \times 10^{-3}$	$\lambda_1 = 0.012$	$\ell = 8.696 \times 10^{-4}$
$\beta_2 = 1.0020 \times 10^{-3}$	$\lambda_2 = 0.031$	$H_0 = 100$
$\beta_3 = 0.8458 \times 10^{-3}$	$\lambda_3 = 0.115$	$k_z = 3.5 \times 10^{-5}$
$\beta_4 = 1.8330 \times 10^{-3}$	$\lambda_4 = 0.301$	$m_z = 2$
$\beta_5 = 0.9682 \times 10^{-3}$	$\lambda_5 = 0.905$	
$\beta_6 = 0.2088 \times 10^{-3}$	$\lambda_6 = 2.760$	

the values in Table 1, system (6) is fully observable and controllable.

The proposed work aims to design a chattering free robust optimal controller, such that the system state $x(t)$ tracks the desired trajectory $x_d(t) \in \mathbb{R}^8$, using estimated state $\hat{x}(t)$. To estimate the unmeasurable states, an observer is designed using sliding mode technique, which is discussed in the next section.

3. Observer design

In case of PHWR, presence of unknown uncertainties in the system may limit the applicability of conventional observers. Hence, sliding mode technique can be used to design an observer. Here, a robust SOISMO based on STA is designed to estimate the unmeasurable delayed neutron precursors' concentration using measurable output power and water level in the ZCCs.

By partitioning the state vector $x(t)$ as

$$x_a(t) = [\delta P \; \delta H]^\top ,$$

and

$$x_b(t) = [\delta C_1 \; \delta C_2 \; \delta C_3 \; \delta C_4 \; \delta C_5 \; \delta C_6]^\top ,$$

system (6) can be expressed as

$$\dot{x}_a(t) = A_{aa} x_a(t) + A_{ab} x_b(t) + B_a u(t), \tag{7}$$

$$\dot{x}_b(t) = A_{ba} x_a(t) + A_{bb} x_b(t) + B_b u(t), \tag{8}$$

$$y(t) = x_a(t). \tag{9}$$

Note that $x_a(t) \in \mathbb{R}^2$ is the measured part of the state vector, $x_b(t) \in \mathbb{R}^6$ is the unmeasured part of the state vector, and $A_{aa} \in \mathbb{R}^{2\times 2}$, $A_{ab} \in \mathbb{R}^{2\times 6}$, $A_{ba} \in \mathbb{R}^{6\times 2}$, $A_{bb} \in \mathbb{R}^{6\times 6}$, $B_a \in \mathbb{R}^2$, $B_b = 0_{[6\times 1]}$ are corresponding sub-matrices of A and B.

The SOISMO for both the subsystems (7) and (8) is designed as [18].

$$\dot{\hat{x}}_a(t) = A_{aa} \hat{x}_a(t) + A_{ab} \hat{x}_b(t) + B_a u(t) + L_1 \overline{x}_a(t) + \nu_d(t) \tag{10}$$

$$\dot{\hat{x}}_b(t) = A_{ba} \hat{x}_a(t) + A_{bb} \hat{x}_b(t) + B_b u(t) + L_2 \nu_d(t). \tag{11}$$

In the above, $\hat{x}_a(t)$ and $\hat{x}_b(t)$ are respectively the estimates of $x_a(t)$ and $x_b(t)$, $\overline{x}_a(t)$ and $\nu_d(t)$ are respectively the estimation error for measured states and the discontinuous observer input which makes the observer robust, given as

$$\overline{x}_a(t) = x_a(t) - \hat{x}_a(t), \tag{12}$$

$$\nu_d(t) = \left[\nu_{d_1}(t)^\top \; \nu_{d_2}(t)^\top\right]^\top , \tag{13}$$

and $L_1 \in \mathbb{R}^{2\times 2}$ and $L_2 \in \mathbb{R}^{6\times 2}$ are the observer gains. In (13), $\nu_d(t)$ is designed based on STA as [13].

$$\nu_{d_i}(t) = -\kappa_{i1} \left|\sigma_{o_i}(t)\right|^{\frac{1}{2}} \mathrm{sign}(\sigma_{o_i}(t)) - \kappa_{i2} \int_0^t \mathrm{sign}(\sigma_{o_i}(\tau)) d\tau \;\; (i = 1, 2.), \tag{14}$$

where

$$\sigma_o(t) = \overline{x}_a(t) + z(t) \in \mathbb{R}^2 \tag{15}$$

is the sliding manifold, κ_{i1} and κ_{i2} $(i = 1, 2.)$ are appropriately designed positive constants to ensure the finite time convergence of the sliding dynamics, and $z(t)$ induces the integral term. The approach for determination of $z(t)$ and the observer gains L_1 ans L_2 are explained in the following.

Let us define the estimation error for the unmeasured states as

$$\overline{x}_b(t) = x_b(t) - \hat{x}_b(t). \tag{16}$$

The error dynamics for the first subsystem, obtained by subtracting (10) from (7), has the form

$$\dot{\overline{x}}_a(t) = A_{aa} \overline{x}_a(t) + A_{ab} \overline{x}_b(t) - L_1 \overline{x}_a(t) - \nu_d(t). \tag{17}$$

According to the equivalent input method, the system in sliding mode behaves as if $\nu_d(t)$ is replaced by its equivalent value $(\nu_d(t))_{eq}$. During sliding $\sigma_o(t) = \dot{\sigma}_o(t) = 0$. Thus, from (15) we get

$$\dot{\sigma}_o(t) = \dot{\overline{x}}_a(t) + \dot{z}(t) = 0. \tag{18}$$

Using (17), (18) becomes

$$A_{aa} \overline{x}_a(t) + A_{ab} \overline{x}_b(t) - L_1 \overline{x}_a(t) - (\nu_d(t))_{eq} + \dot{z}(t) = 0. \tag{19}$$

Let us define

$$\dot{z}(t) = -A_{aa} \overline{x}_a(t) + L_1 \overline{x}_a(t).$$

Then,

$$z(t) = -\int_0^t (A_{aa} \overline{x}_a(\tau) - L_1 \overline{x}_a(\tau)) \; d\tau + z(0),$$

and, from (15), at $t = 0$,

$$z(0) = -\overline{x}_a(0).$$

From (19), the equivalent input can be obtained as

$$(\nu_d(t))_{eq} = A_{ab} \overline{x}_b(t). \tag{20}$$

Using (20), (17) becomes

$$\dot{\overline{x}}_a(t) = (A_{aa} - L_1 I_2) \overline{x}_a(t), \tag{21}$$

where I_2 denotes an identity matrix of order 2. Since the pair (A_{aa}, I_2) is always observable, it is possible to choose appropriate gain L_1 so that the sliding occurs in (17) along the sliding manifold $\sigma_o(t) = 0$ and the desired rate of decay of $\overline{x}_a$ can be obtained. Similarly, the error dynamics for the second subsystem obtained by subtracting (11) from (8), has the form

$$\dot{\overline{x}}_b = A_{ba}\overline{x}_a + A_{bb}\overline{x}_b - L_2(v_d(t))_{eq}\dot{\overline{x}}_b = A_{ba}\overline{x}_a + (A_{bb} - L_2A_{ab})\overline{x}_b. \tag{22}$$

It can be shown that if system (6) (the pair (A,M)) is observable then the pair (A_{bb}, A_{ab}) is also observable [16] and, therefore, by appropriate choice of gain L_2 the desired rate of decay of $\overline{x}_b(t)$ can be obtained. Now, with the estimated states $\widehat{x}(t) = [\widehat{x}_a(t)^\top \ \widehat{x}_b(t)^\top]^\top$, the proposed OSOISMC is designed, which is discussed in the next section.

4. Controller design

Let us consider the system (6). When it is affected by bounded matched uncertainties, it can be represented as

$$\begin{aligned}\dot{x}(t) &= Ax(t) + B(u(t) + \xi(t)),\\ y(t) &= Mx(t),\end{aligned} \tag{23}$$

where $\xi(t)$ represents unknown bounded lumped uncertainties. Control input $u(t)$ is designed as

$$u(t) = u_c(t) + u_d(t), \tag{24}$$

where $u_c(t)$ is the nominal continuous control responsible for achieving the desired performance for the nominal system and $u_d(t)$ is the discontinuous control that tackles the uncertainties and disturbances. With (24), system (23) can be written as

$$\begin{aligned}\dot{x}(t) &= Ax(t) + B(u_c(t) + u_d(t) + \xi(t)),\\ y(t) &= Mx(t).\end{aligned} \tag{25}$$

In order to track the desired trajectory with minimum control input, the nominal control $u_c(t)$ is designed using LQT technique and to overcome the uncertainties present in the system, the discontinuous control $u_d(t)$ is designed using SMC technique, as elaborated in the following subsections.

4.1. Design of nominal control

Continuous control $u_c(t)$ is designed considering only nominal system. Neglecting uncertainties, (25) can be written as

$$\dot{x}(t) = Ax(t) + Bu_c(t). \tag{26}$$

Let us define the tracking error vector as

$$e(t) = x(t) - x_d(t), \tag{27}$$

where $x_d(t)$ denotes the desired trajectory. Note that the tracking error $e(t)$ is not directly measurable since it depends on the state vector $x(t)$. Hence, for the design of controller estimated state vector $\widehat{x}(t)$ is used. Thus, estimated tracking error vector $\widehat{e}(t)$ is obtained as

$$\widehat{e}(t) = \widehat{x}(t) - x_d(t). \tag{28}$$

To apply LQT design technique to the system (26), a quadratic performance index J is defined as

$$J = \frac{1}{2}\int_0^\infty \left(\widehat{e}(\tau)^\top Q\widehat{e}(\tau) + u_c(\tau)^\top Ru_c(\tau)\right)d\tau \ , \tag{29}$$

where $Q \geq 0 \in \mathbb{R}^{8\times 8}$ and $R > 0 \in \mathbb{R}$, are appropriate weighing matrices.

According to the LQT control theory, the nominal control $u_c(t)$ minimizing the cost function J is given by [8].

$$\begin{aligned}u_c(t) &= -R^{-1}B^\top (S\widehat{x}(t) - g(t))\\ &= -K\widehat{x}(t) + R^{-1}B^\top g(t),\end{aligned} \tag{30}$$

where $K = R^{-1}B^\top S$ is the Kalman gain, $S > 0$ is the symmetric matrix which satisfies the continuous time algebraic Riccati equation

$$A^\top S + SA + Q - SBR^{-1}B^\top S = 0, \tag{31}$$

and $g(t)$ is the solution of

$$\dot{g}(t) = \left(SBR^{-1}B^\top - A^\top\right)g(t) - Qx_d(t), \ g(\infty) = 0_{[8\times 1]}. \tag{32}$$

Substituting the value of $u_c(t)$ from (30) in (26), the closed loop system dynamics is given by

$$\dot{x}(t) = (A - BK)x(t) + R^{-1}B^\top \ g(t). \tag{33}$$

Thus, from (33) it is clear that with the control $u_c(t)$ the nominal system states $x(t)$ asymptotically tracks the desired trajectory $x_d(t)$. However, the performance of the nominal control may degrade when applied to uncertain system (23) directly. Hence, to improve the closed loop system performance in the presence of uncertainties, the nominal control is combined with the robust discontinuous control.

4.2. Design of discontinuous control

Let us define an integral sliding surface $\sigma_c(t) \in \mathbb{R}$ which retains the nominal closed loop performance as

$$\sigma_c(t) = G\left[\widehat{x}(t) - \widehat{x}(0) - \int_0^t (A\widehat{x}(\tau) + Bu_c(\tau))\, d\tau\right], \tag{34}$$

where projection matrix $G \in \mathbb{R}^{1\times 8}$ is design freedom. The term $-\widehat{x}(0)$ achieves the property that $\sigma_c(0) = 0$, hence the sliding mode will exist from the very beginning of the system response (no reaching phase) and system becomes more robust towards uncertainties as compared to conventional SMC techniques.

In this work, G is chosen as

$$G = \left(B^\top B\right)^{-1}B^\top. \tag{35}$$

To avoid chattering effect, the discontinuous control $u_d(t)$ is designed based on STA as [13].

$$u_d(t) = -\mu_1\left|\sigma_c(t)\right|^{\frac{1}{2}}\text{sign}(\sigma_c(t)) - \mu_2\int_0^t \text{sign}(\sigma_c(\tau))\, d\tau, \tag{36}$$

where μ_1 and μ_2 are appropriately designed positive constants, and selection of their values is discussed later in the next subsection.

Now, substituting (30) and (36) in (24), the total control $u(t)$ is obtained as

$$\begin{aligned}u(t) = -K\widehat{x}(t) + R^{-1}B^\top g(t) - \mu_1\left|\sigma_c(t)\right|^{\frac{1}{2}}\text{sign}(\sigma_c(t))\\ -\mu_2\int_0^t \text{sign}(\sigma_c(\tau))d\tau.\end{aligned} \tag{37}$$

4.3. Stability analysis

From (34), the sliding dynamics is given by

$$\dot{\sigma}_c(t) = G\left(\dot{\widehat{x}}(t) - A\widehat{x}(t) - Bu_c(t)\right) = G(A\widehat{x}(t) + Bu_c(t) + Bu_d(t) + B\xi(t) - A\widehat{x}(t) - Bu_c(t)) = u_d(t) + \xi(t)$$
$$= -\mu_1 \left|\sigma_c(t)\right|^{\frac{1}{2}}\mathrm{sign}(\sigma_c(t)) - \mu_2 \int_0^t \mathrm{sign}(\sigma_c(\tau))d\tau + \xi(t). \quad (38)$$

Let us assume that the time derivative of lumped uncertainty $\xi(t)$ is also bounded *i.e.*,

$$|\dot{\xi}(t)| \leq \Upsilon. \quad (39)$$

Thus, the sliding dynamics (38) can be represented as

$$\dot{z}_1(t) = -\mu_1 \left|z_1(t)\right|^{\frac{1}{2}}\mathrm{sign}(z_1(t)) + z_2(t), \quad (40)$$

and

$$\dot{z}_2(t) = -\mu_2 \mathrm{sign}(z_1(t)) + \Upsilon. \quad (41)$$

Let us define a vector $\Sigma = \left[\left|z_1(t)\right|^{\frac{1}{2}}\mathrm{sign}(z_1(t)) \quad z_2(t)\right]^\top$. Thus, the time derivative of Σ is given by

$$\dot{\Sigma} = \frac{1}{\left|z_1(t)\right|^{\frac{1}{2}}} A_c \Sigma, \quad (42)$$

where

$$A_c = \begin{bmatrix} -\frac{1}{2}\mu_1 & \frac{1}{2} \\ -\mu_2 + \Upsilon & 0 \end{bmatrix}. \quad (43)$$

Now, choose the Lyapunov function as [19].

$$V_c(t) = \Sigma^\top S_c \Sigma, \quad (44)$$

where S_c is a symmetric positive definite matrix, defined as

$$S_c = \frac{1}{2}\begin{bmatrix} \mu_1^2 + 4\mu_2 & -\mu_1 \\ -\mu_1 & 2 \end{bmatrix}. \quad (45)$$

The time derivative of Lyapunov function (44) can be computed similar to Ref. [20] and [21] as

$$\dot{V}_c(t) = -\frac{1}{\left|z_1(t)\right|^{\frac{1}{2}}} \Sigma^\top Q_c \Sigma, \quad (46)$$

where Q_c is a positive definite matrix given as

$$Q_c = \frac{\mu_1}{2}\begin{bmatrix} \mu_1^2 + 2\mu_2 + 2\Upsilon & -\left(\mu_1 + \frac{2\Upsilon}{\mu_1}\right) \\ -\left(\mu_1 + \frac{2\Upsilon}{\mu_1}\right) & 1 \end{bmatrix}. \quad (47)$$

Matrices S_c and Q_c are related by the algebraic Lyapunov equation

$$A_c^\top S_c + S_c A_c = -Q_c. \quad (48)$$

To ensure that matrix Q_c is positive definite, the gains μ_1 and μ_2 are selected as

$$\mu_1 > 0 \text{ and } \mu_2 > \Upsilon + 2\left(\frac{\Upsilon}{\mu_1}\right)^2. \quad (49)$$

Employing the fact that $\left|z_1(t)\right|^{\frac{1}{2}} \leq \|\Sigma\|$, (46) can be written as

$$\dot{V}_c(t) \leq -\lambda_{min}(Q_c)\|\Sigma\|. \quad (50)$$

It is evident from (50) that the Lyapunov function (44) will decrease gradually, which implies that the system state will track the desired trajectory in a finite time.

5. Simulation results and discussion

For the PHWR, the proposed observer based robust optimal control scheme is designed to achieve stable response as well as adequate degree of robustness in the presence of uncertainties and disturbances. Values of design parameters of the proposed observer based control scheme are selected by performing large number of simulation experiments and those values, which produce the best transient and steady state performance, are chosen, as given in Table 2. Furthermore, desired trajectory $x_d(t)$ is generated from steady state equations using demand power as reference.

First, performance of the proposed observer in the presence of measurement noise is analyzed. An additive white Gaussian noise has been added to the measurement (P) such that the signal to noise ratio is 50 dB. It is assumed that the reactor is operating at steady state full power and the control input to the system is zero. All the state variables are in equilibrium with steady state power. A

Table 2
Values of different design parameters.

$$L_1 = \text{diag.}[10, 1]$$
$$L_2 = \begin{bmatrix} 0.3 & 0.2 & 0.3 & 0.2 & 0.2 & 0.2 \\ 0.1 & 0.1 & 0.1 & 0.1 & 0.1 & 0.1 \end{bmatrix}^{\top}$$
$$\kappa = \begin{bmatrix} 1 & 0.001 \\ 0.1 & 0.001 \end{bmatrix}$$
$$Q = \text{diag.}[100, 0.001, 0.001, 0.001, 0.001, 0.001, 0.001, 0.001]$$
$$R = 3$$
$$\mu_1 = 0.1$$
$$\mu_2 = 3.1 \times 10^{-2}$$

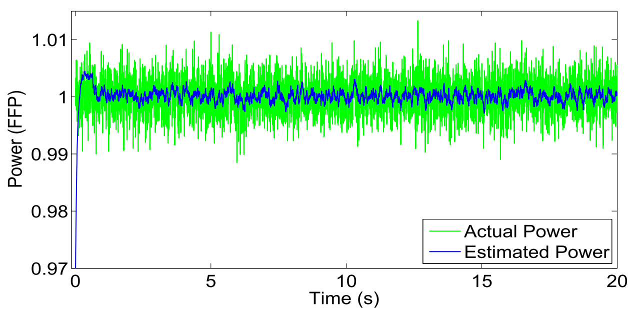

Fig. 1. Comparison of actual power and estimated power.

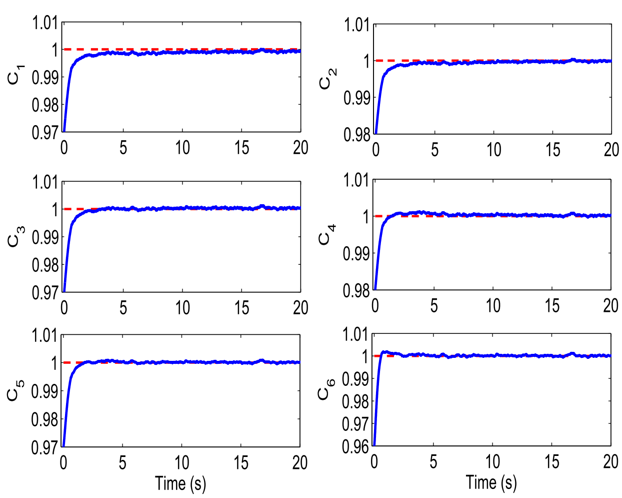

Fig. 2. Comparison of actual precursors' concentration and estimated precursors' concentration.

difference in initial condition of estimated states and the actual states is also considered, by assuming the initial condition for the estimated states as $[0.97, 0, 0.97, 0.98, 0.97, 0.98, 0.97, 0.96]^{\top}$. Comparison of actual output and the estimated output is shown in Fig. 1. It can be observed that the proposed observer exhibits good filtering capabilities under noisy conditions. Variation of estimated delayed neutron precursors' concentration is shown in Fig. 2.

In another simulation study, robustness of the proposed controller in the presence of external disturbance is evaluated. It is assumed that initially the reactor is operating in steady state condition at the power level of 0.9 *FFP*. At $t = 20\ s$, the demand power is reduced from 0.9 *FFP* to 0.85 *FFP* at the rate of 0.002 *FFP* /*s*. A sinusoidal external disturbance with peak amplitude $\pm 10\ mV$ and frequency 0.1 *rad* /*s* is considered throughout the system response

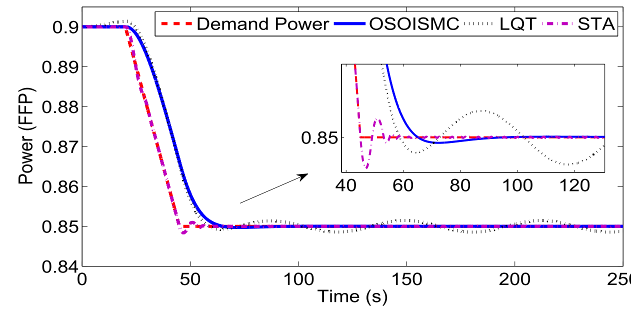

Fig. 3. Total reactor power with OSOISMC, LQT controller and STA based controller.

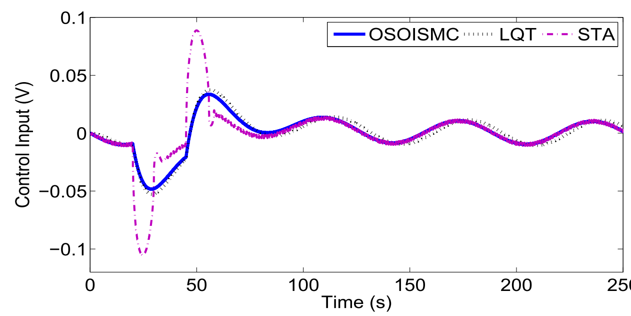

Fig. 4. Control input for OSOISMC, LQT controller and STA based controller.

in the control input to ZCCs. The simulation results obtained by applying the proposed controller are compared with those obtained by using the LQT controller and the controller designed based on STA. In STA based controller the sliding surface is designed as $\sigma_c(t) = P(t) - P_d(t)$ and the values of μ_1 and μ_2 are selected as 1.5 and 3.1×10^{-2}, respectively. The LQT controller is designed by making $u_d(t) = 0$ in (24). Variation of total reactor power with three different controllers are shown in Fig. 3. It can be observed that the proposed controller and the controller based on STA successfully tracks the variation in demand power in spite of the presence of disturbance in the input while LQT controller fails to maintain it. The proposed controller and STA based controller are found to be robust towards disturbances that lie in the input channel provided the discontinuous control gains satisfy the condition (49). Time variation of control input for OSOISMC, LQT controller and STA based controller are shown in Fig. 4. Comparison of control energy calculated by using the 2-norm method, for above three controllers are given in Table 3. It can be seen that the OSOISMC spend less control energy as compared to the LQT controller and STA based controller while tackling with disturbances present in the system. The control energies of three different controllers without considering uncertainty and disturbance are further compared. In this case the control energy spent by OSOISMC is in comparison with LQT controller. Fig. 5 shows the

Table 3
Comparison of control energies.

	Method	Control Energy
with disturbance	Proposed SOISMC	2.4849
	LQT controller	2.7286
	STA based controller	4.6235
without disturbance	Proposed SOISMC	2.2995
	LQT controller	2.2933
	STA based controller	4.3344

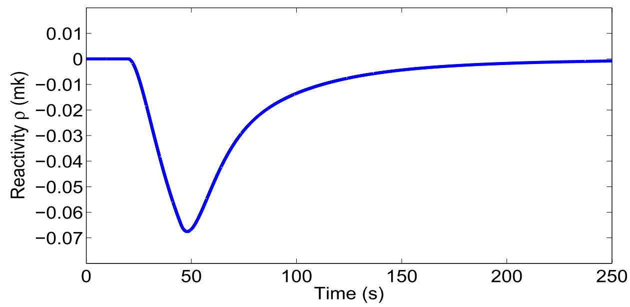

Fig. 5. Change in reactivity for OSOISMC.

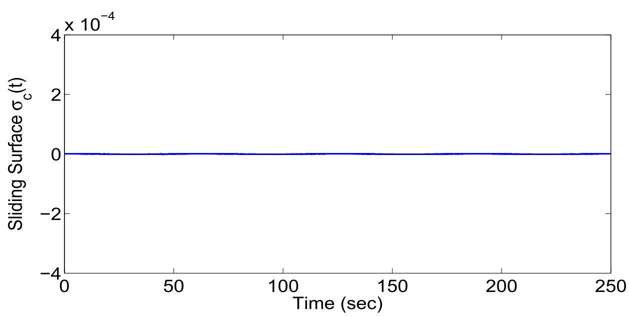

Fig. 6. Sliding surface for OSOISMC.

change in reactivity for OSOISMC. Variation of sliding surface is shown in Fig. 6.

Finally, effectiveness of the proposed observer based control scheme in the presence of parametric uncertainty is evaluated. It is assumed that the reactor is operating in steady state condition at the power level of 0.5 *FFP*. Mismatch between initial conditions of estimated states and the actual states is considered by assuming the initial condition for the estimated states as $[0.52, 0, 0.54, 0.53, 0.54, 0.52, 0.53, 0.52]^\top$. As a parametric uncertainty the system parameters (β_i and λ_i) are simultaneously perturbed hypothetically throughout the system response from their initial values with a sinusoid of peak amplitude $\pm 20\%$ and frequency 20 *rad* /*s*. At $t = 50$ *s*, the demand power is increased from 0.5 *FFP* to 0.7 *FFP* at the rate of 0.005 *FFP* /*s*. During these transients, total power varies as shown in Fig. 7. It can be observed that the total power tracks the demand power asymptotically. This shows that the performance of the proposed control scheme is not much affected by the parametric uncertainties. Furthermore, to demonstrate the efficacy of the proposed sliding mode observer, comparison of actual states and the estimated states for a initial

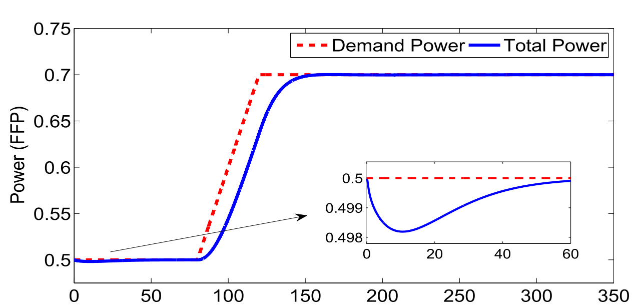

Fig. 7. Total reactor power.

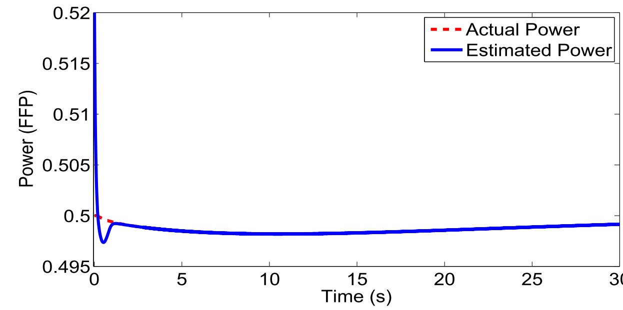

Fig. 8. Comparison of actual power and estimated power.

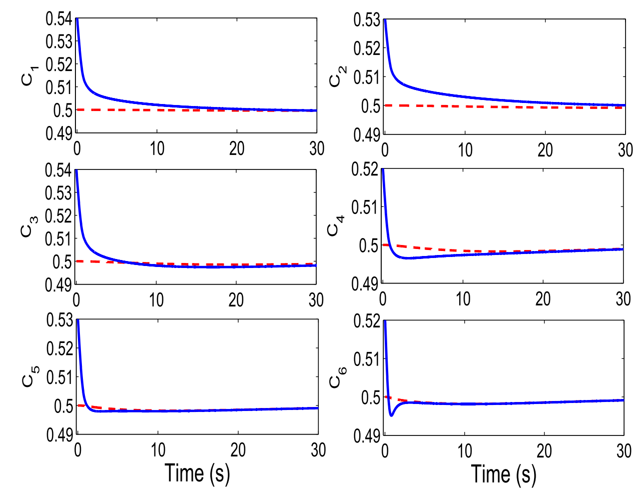

Fig. 9. Comparison of actual precursors' concentration and estimated precursors' concentration.

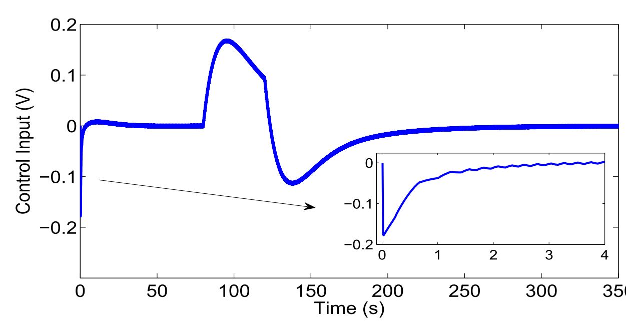

Fig. 10. Control input to ZCC.

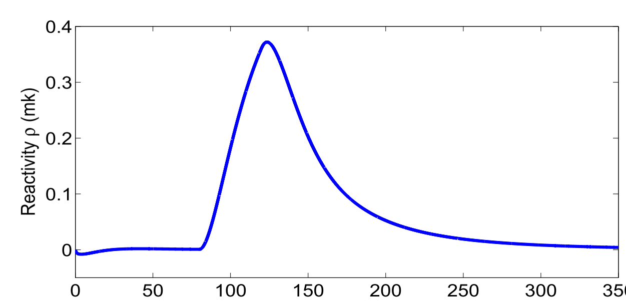

Fig. 11. Change in reactivity.

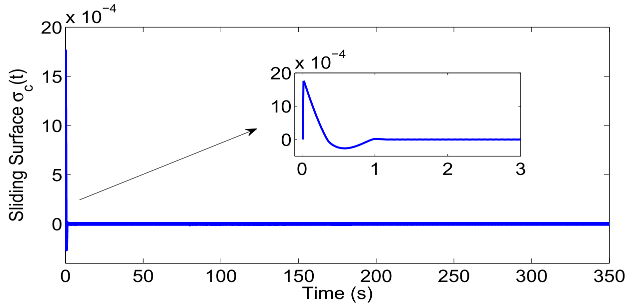

Fig. 12. Sliding surface.

period of 30 *s* are shown in Figs. 8 and 9, respectively. It can be observed that the estimated state variables follows very closely the actual state variables. Variation of control input and change in reactivity due to it are shown in Figs. 10 and 11, respectively. Variation of sliding surface is shown in Fig. 12.

6. Conclusions

In this paper, a second order integral sliding mode observer and controller based on the super-twisting algorithm are designed to control the total power of a nuclear reactor. The proposed controller is realized by combining an optimal controller with a second order integral sliding mode controller. Stability of the proposed controller is proved with the help of strict Lyapunov function. An observer is designed to estimate the unmeasured delayed neutron precursors' concentration. Its sensitivity against the measurement noise is studied. Simulation results show that the proposed control scheme provides satisfactory tracking performance in the presence of parametric uncertainties and external disturbance, and the proposed observer exhibits good filtering capabilities under noisy conditions.

Appendix A. Supplementary data

Supplementary data to this article can be found online at https://doi.org/10.1016/j.net.2019.08.013.

References

[1] G.D. Reddy, B. Bandyopadhyay, A.P. Tiwari, Multirate output feedback based sliding mode spatial control for a large PHWR, IEEE Trans. Nucl. Sci. 54 (6) (Dec 2007) 2677–2686.
[2] R.K. Munje, B.M. Patre, S.R. Shimjith, A.P. Tiwari, Sliding mode control for spatial stabilization of advanced heavy water reactor, IEEE Trans. Nucl. Sci. 60 (4) (Aug 2013) 3040–3050.
[3] P.V. Surjagade, A.P. Tiwari, S.R. Shimjith, Robust optimal integral sliding mode controller for total power control of large PHWRs, IEEE Trans. Nucl. Sci. 65 (7) (July 2018) 1331–1344.
[4] M. Eom, D. Chwa, D. Baang, Robust disturbance observer-based feedback linearization control for a research reactor considering a power change rate constraint, IEEE Trans. Nucl. Sci. 62 (3) (June 2015) 1301–1312.
[5] G.R. Ansarifar, M. Rafiei, Second-order sliding-mode control for a pressurized water nuclear reactor considering the xenon concentration feedback, Nucl. Eng. Technol. 47 (1) (2015) 94–101.
[6] S. Qaiser, A. Bhatti, M. Iqbal, R. Samar, J. Qadir, Model validation and higher order sliding mode controller design for a research reactor, Ann. Nucl. Energy 36 (1) (2009) 37–45.
[7] M.Z. Nejad, G. Ansarifar, Adaptive observer based adaptive control for P.W.R nuclear reactors during load following operation with bounded xenon oscillations using lyapunov approach, Ann. Nucl. Energy 121 (2018) 382–405.
[8] D.S. Naidu, in: R.C. Dorf (Ed.), Optimal Control Systems, CRC Press, Inc., Boca Raton, FL, USA, 2002.
[9] L. Fridman, A. Poznyak, F. Bejarano, Robust Output LQ Optimal Control via Integral Sliding Modes, March 2014.
[10] C. Edwards, S.K. Spurgeon, Sliding Mode Control: Theory and Applications, Taylor and Francis, 1998.
[11] V. Utkin, J. Shi, Integral sliding mode in systems operating under uncertainty conditions, in: Proceedings of 35th IEEE Conference on Decision and Control vol. 4, Dec 1996, pp. 4591–4596.
[12] J.J.E. Slotine, W. Li, Applied Nonlinear Control, Prentice Hall, Englewood Cliffs, NJ, 1991. Pearson.
[13] A. Levant, Sliding order and sliding accuracy in sliding mode control, Int. J. Control 58 (6) (1993) 1247–1263.
[14] S.R. Shimjith, A.P. Tiwari, B. Bandyopadhyay, Design of fast output sampling controller for three-time-scale systems: application to spatial control of advanced heavy water reactor, IEEE Trans. Nucl. Sci. 58 (6) (Dec 2011) 3305–3316.
[15] F. Chen, M.W. Dunnigan, Comparative study of a sliding-mode observer and Kalman filters for full state estimation in an induction machine, IEE Proc. Electr. Power Appl. 149 (1) (Jan 2002) 53–64.
[16] S. Drakunov, V. Utkin, Sliding mode observers. tutorial, in: Proceedings of 34th IEEE Conference on Decision and Control 4, Dec 1995, pp. 3376–3378.
[17] G. Ablay, Robust reactivity, neutron source, and precursor estimators for nuclear reactors, Nucl. Eng. Des. 265 (2013) 526–533.
[18] E. Jimenez-Rodriguez, E. Mejia-Estrada, O. Jaramillo, J.D. Sanchez-Torres, An integral sliding mode observer for linear systems, in: XVII Latin American Conference Of Automatic Control, IFAC, Medellin, Colombia, 2016, pp. 143–147.
[19] J.J. Rath, M. Defoort, H.R. Karimi, K.C. Veluvolu, Output feedback active suspension control with higher order terminal sliding mode, IEEE Trans. Ind. Electron. 64 (2) (Feb 2017) 1392–1403.
[20] J. Davila, L. Fridman, A. Levant, Second-order sliding-mode observer for mechanical systems, IEEE Trans. Autom. Control 50 (11) (Nov 2005) 1785–1789.
[21] J.A. Moreno, M. Osorio, Strict Lyapunov functions for the super-twisting algorithm, IEEE Trans. Autom. Control 57 (4) (April 2012) 1035–1040.